Supplement of Biogeosciences, 20, 1963–1977, 2023
https://doi.org/10.5194/bg-20-1963-2023-supplement

Biogeosciences Open Access EGU

Supplement of

Considerations for hypothetical carbon dioxide removal via alkalinity addition in the Amazon River watershed

Linquan Mu et al.

Correspondence to: Linquan Mu (mulinquan@gmail.com)

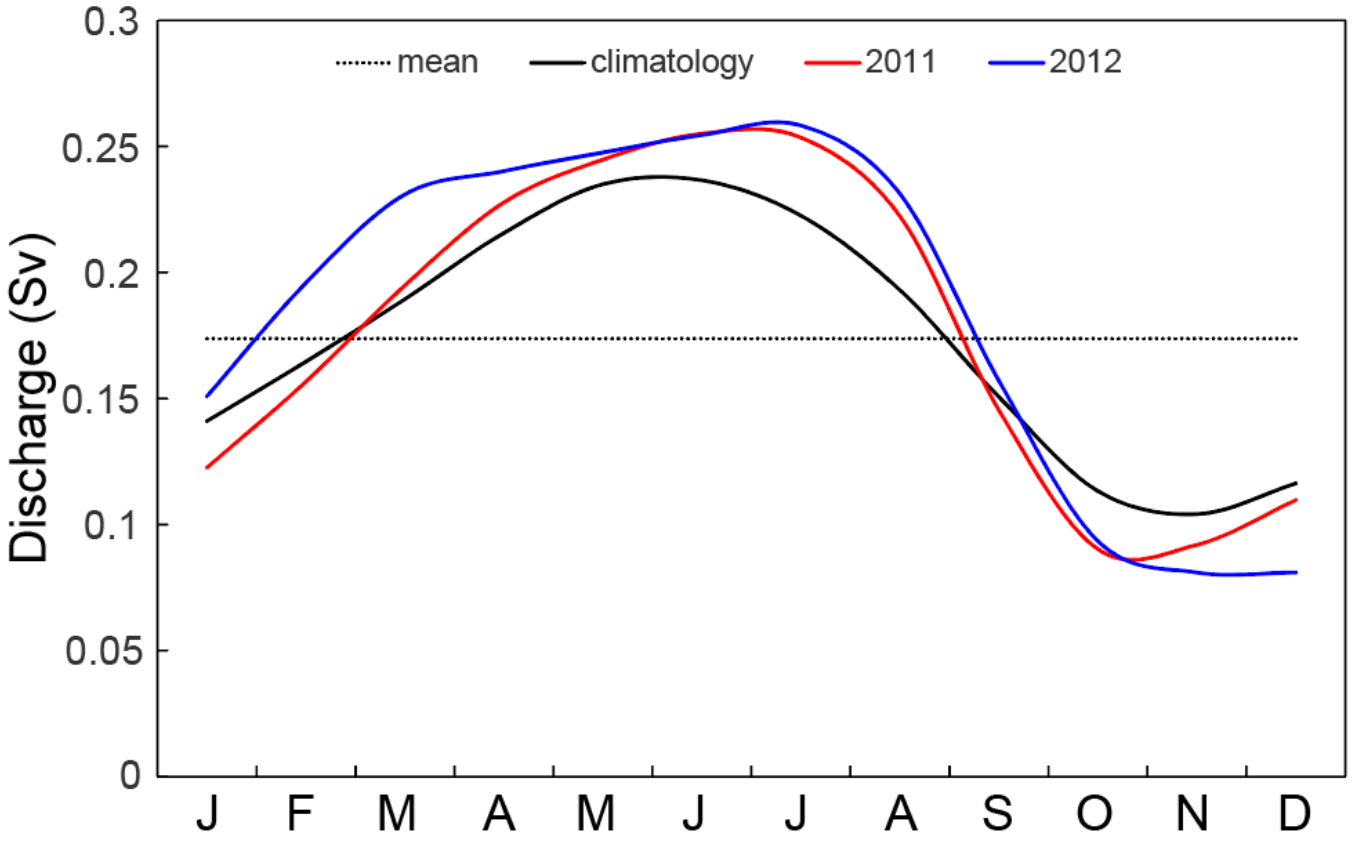

Figure S1. Monthly discharge of the Amazon River (Sv; 1 Sv = 10^6 m^3 s^{-1}) at the Óbidos gauge station (~650 km upriver from the mouth) in 2011 (red line), 2012 (blue line), and climatology averaged over 1968–2012 (black line), in reference to the mean annual discharge 1968–2012 (dotted line).

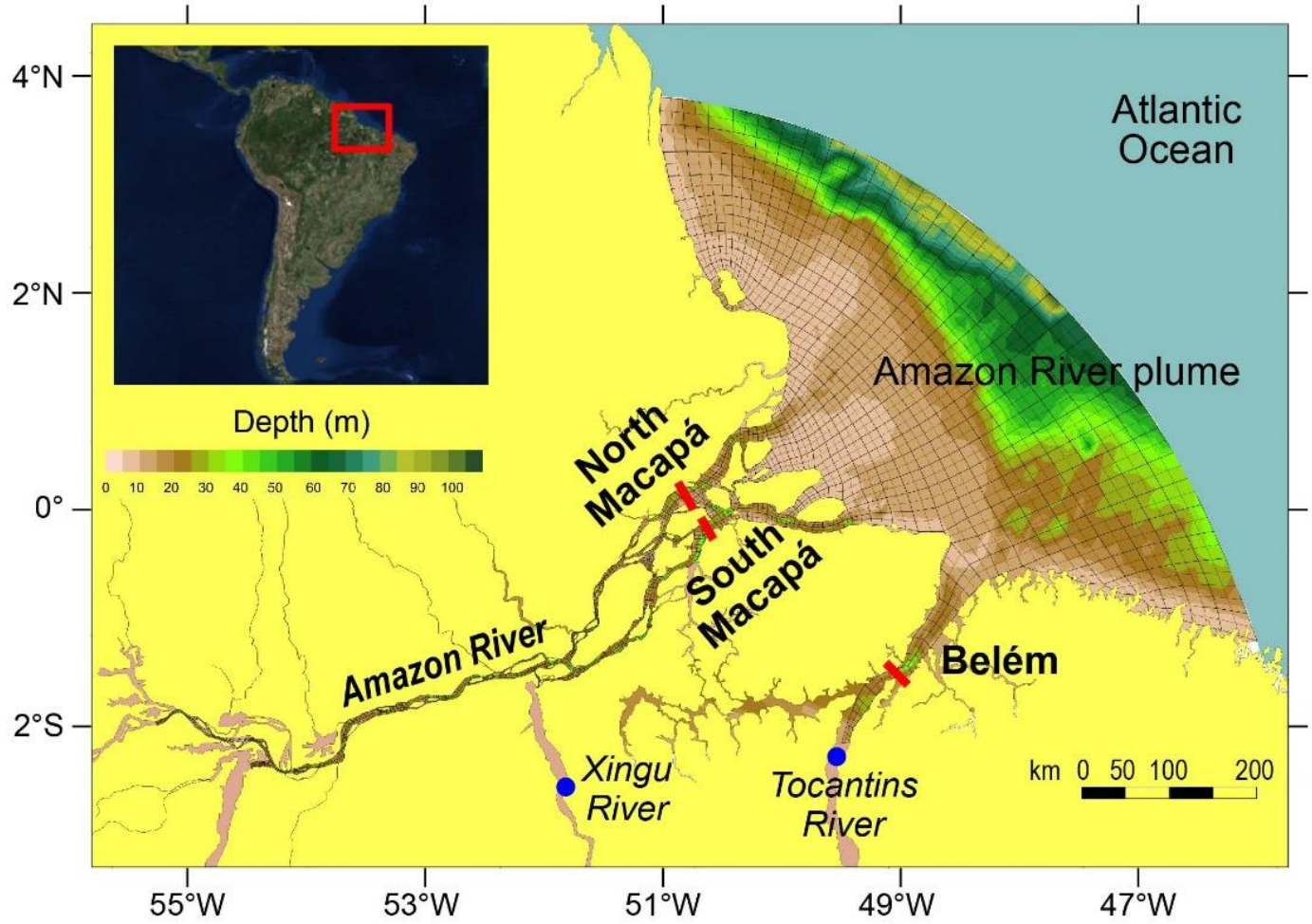

Figure S2. Map of the Amazon River lower reach. Geochemical surveys (in particular, river TA and DIC measurements) were conducted at the outer gateways (North Macapá, South Macapá, and Belém) during the September 2011 and July 2012 *River Ocean Continuum of the Amazon* (ROCA) project. This figure is reproduced from Ward et al. (2015) and Mu et al. (in revision).

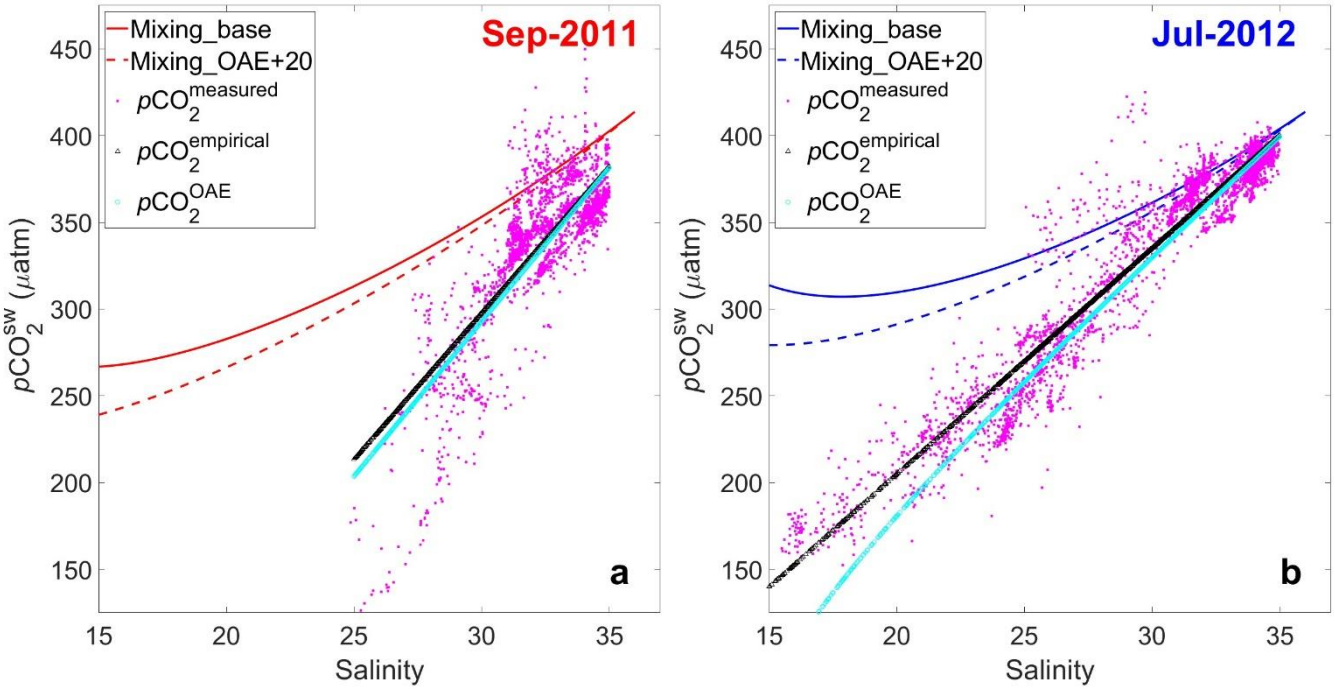

Figure S3. Surface pCO_2 in the Amazon River plume at 15 < salinity < 35 and river-ocean mixing curve before and after the TA perturbation at the mouth for (a) September 2011 and (b) July 2012. TA perturbation strength is 20 μmol kg^{-1}. The TA and DIC for the baseline mixing curves (solid red and blue lines) are calculated from the river and ocean endmember values, from which $pCO_2^{mix\_base}$ at each salinity stamp is calculated using the CO2SYS program. The dashed lines show the OAE-perturbed mixing curve at ΔTA = 20 μmol kg^{-1}. Black triangle markers show the empirical pCO_2 ($pCO_2^{empirical}$) at the plume surface computed from satellite-derived salinity and measured pCO_2 ($pCO_2^{measured}$; magenta dots) versus salinity regression, and open cyan circles represent the OAE-perturbed plume pCO_2 (pCO_2^{OAE}) at ΔTA = 20 μmol kg^{-1}. Salinity as low as 15 was observed in the July 2012 survey, while no salinity under 25 was recorded during the September 2011 cruise.

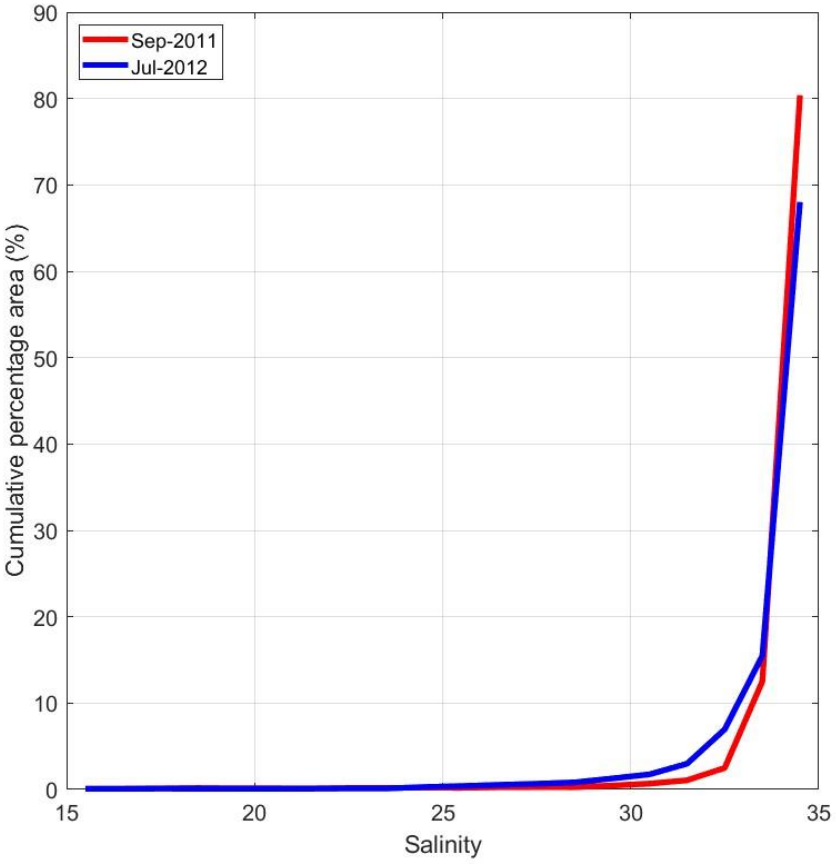

Figure S4. Cumulative percentage area (%) of the Amazon River plume across salinity bands within 15 < SSS < 35 for September 2011 (red) and July 2012 (blue). Note that the freshest part of the plume (SSS < 15) is excluded from the total area to compute the percentages. This figure is reproduced from Mu et al. (2021).

30

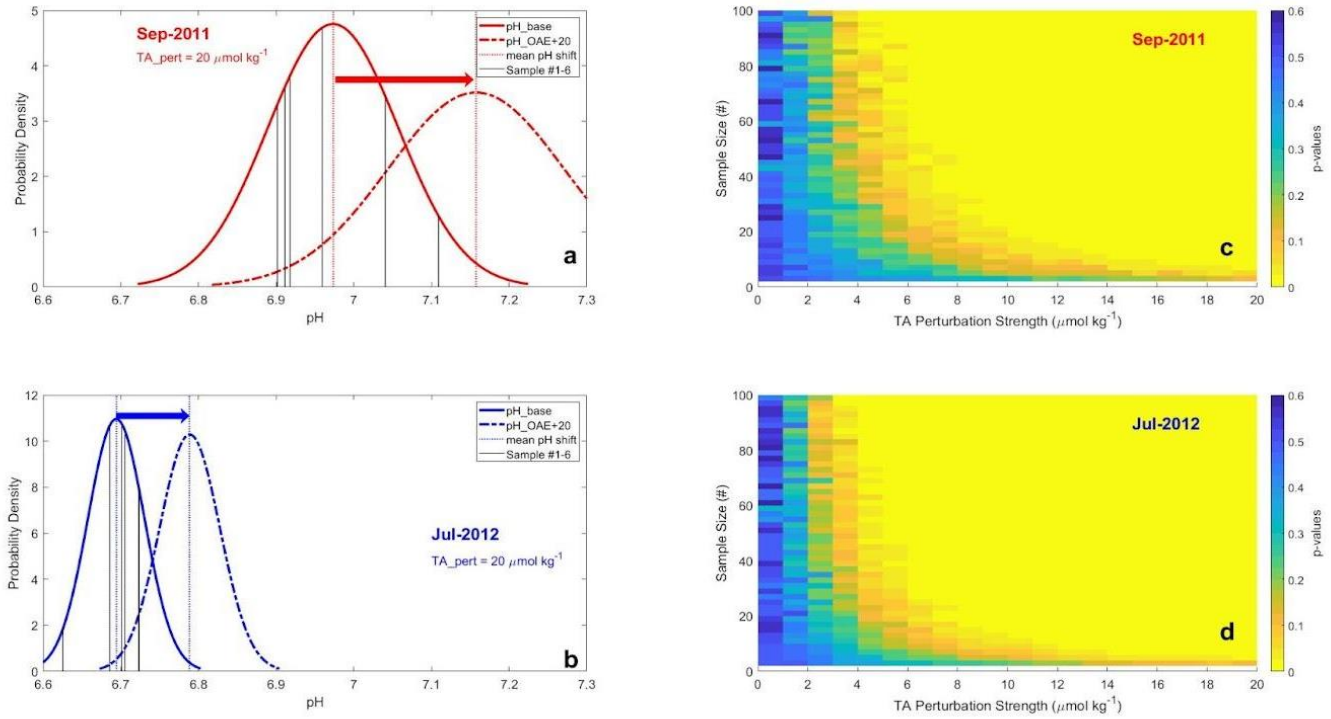

Figure S5. Detectability of OAE-induced pH variation in the North Macapá gateway relative to its background variability. (**a**)(**b**). The theoretical shift of pH (μmol kg^{-1}) means and distributions for September 2011 and July 2012 due to the addition of 20 μmol kg^{-1} of TA at the Amazon River mouth. Black lines indicate baseline pH calculated by baseline TA and DIC at the river mouth. The mean and standard deviations of pH in the perturbation scenarios (dash-dot lines) are calculated from perturbed TA and DIC values. (**c**)(**d**). The p-value plots from t-tests simulated between baseline and perturbed pH induced by TA perturbation scenarios at various sample sizes and TA perturbation strengths for September 2011 and July 2012. Areas in yellow ($p < 0.1$) indicate conditions where an analyst would conclude that the TA perturbation was detected relative to the baseline condition with 90% certainty.

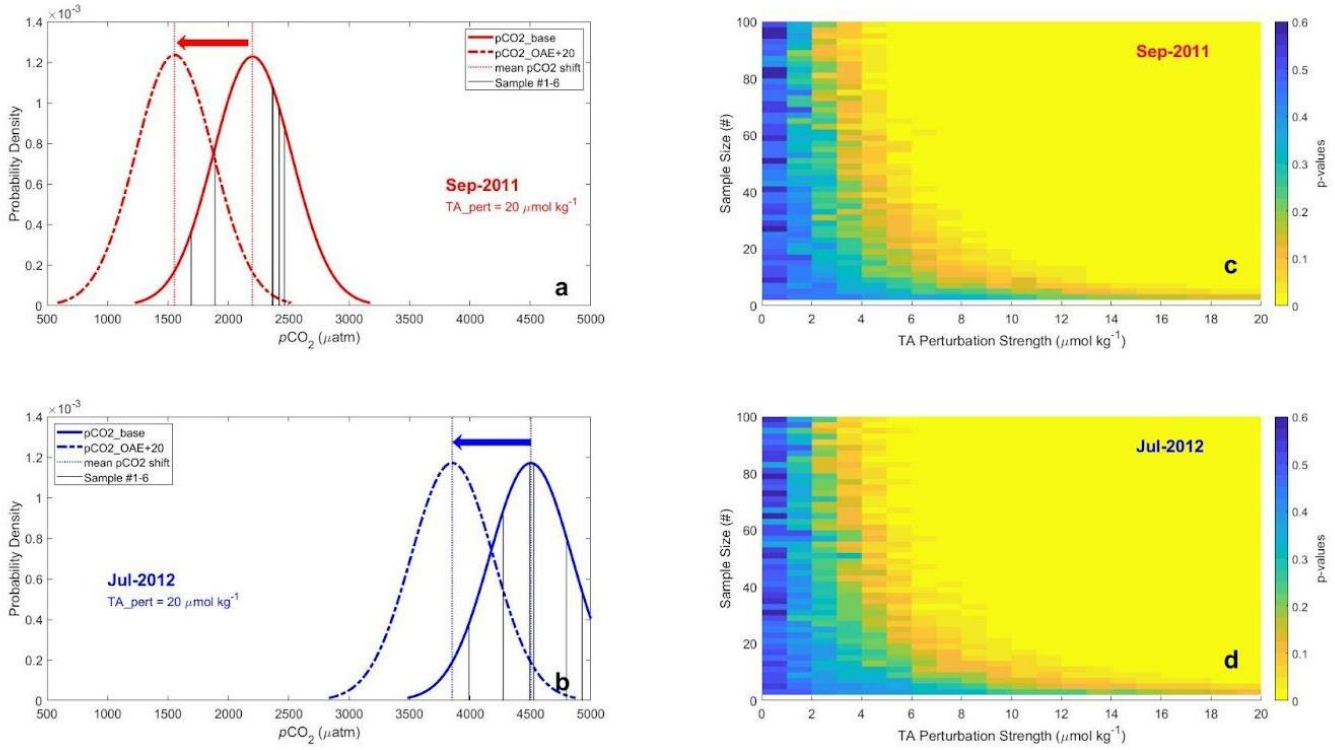

Figure S6. Detectability of OAE-induced pCO_2 variation in the North Macapá gateway relative to its background variability. (**a**)(**b**). The theoretical shift of pCO_2 (μatm) means and distributions for September 2011 and July 2012 due to the addition of 20 μmol kg^{-1} of TA at the Amazon River mouth. Black lines indicate the baseline pCO_2 calculated by baseline TA and DIC at the river mouth. The mean and standard deviations of pCO_2 in the perturbation scenarios (dash-dot lines) are calculated from perturbed TA and DIC values. (**c**)(**d**). The p-value plots from t-tests simulated between baseline and perturbed pCO_2 induced by TA perturbation scenarios at various sample sizes and TA perturbation strengths for September 2011 and July 2012. Areas in yellow ($p < 0.1$) indicate conditions where an analyst would conclude that the TA perturbation was detected relative to the baseline condition with 90% certainty.

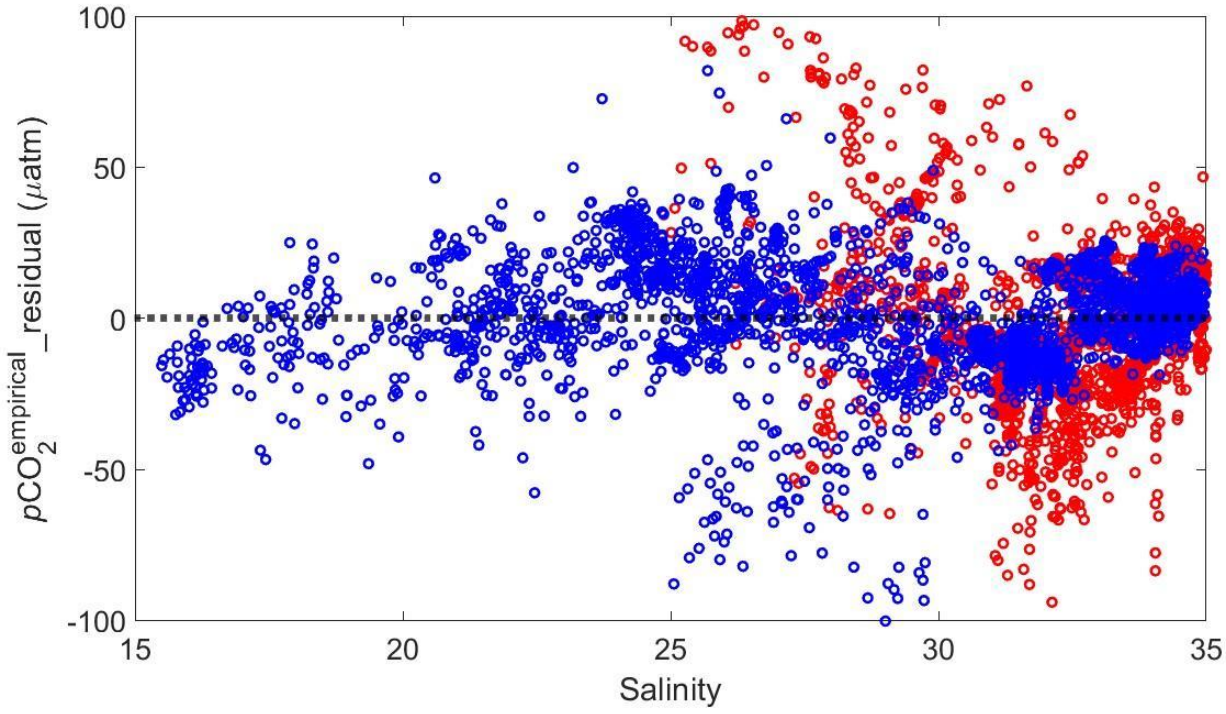

Figure S7. The residual of empirical pCO_2 relative to the measured pCO_2 at the same salinity across the salinity spectrum of 15 < SSS < 35 for September 2011 (red circle) and July 2012 (blue circle). Note that $pCO_2^{empirical}$_residual = $pCO_2^{empirical}$ – $pCO_2^{measured}$ at 15 < SSS < 35. $pCO_2^{empirical}$ is calculated from cruise-specific $pCO_2^{measured}$ versus SSS regression at a satellite-derived salinity (Mu et al., 2021).

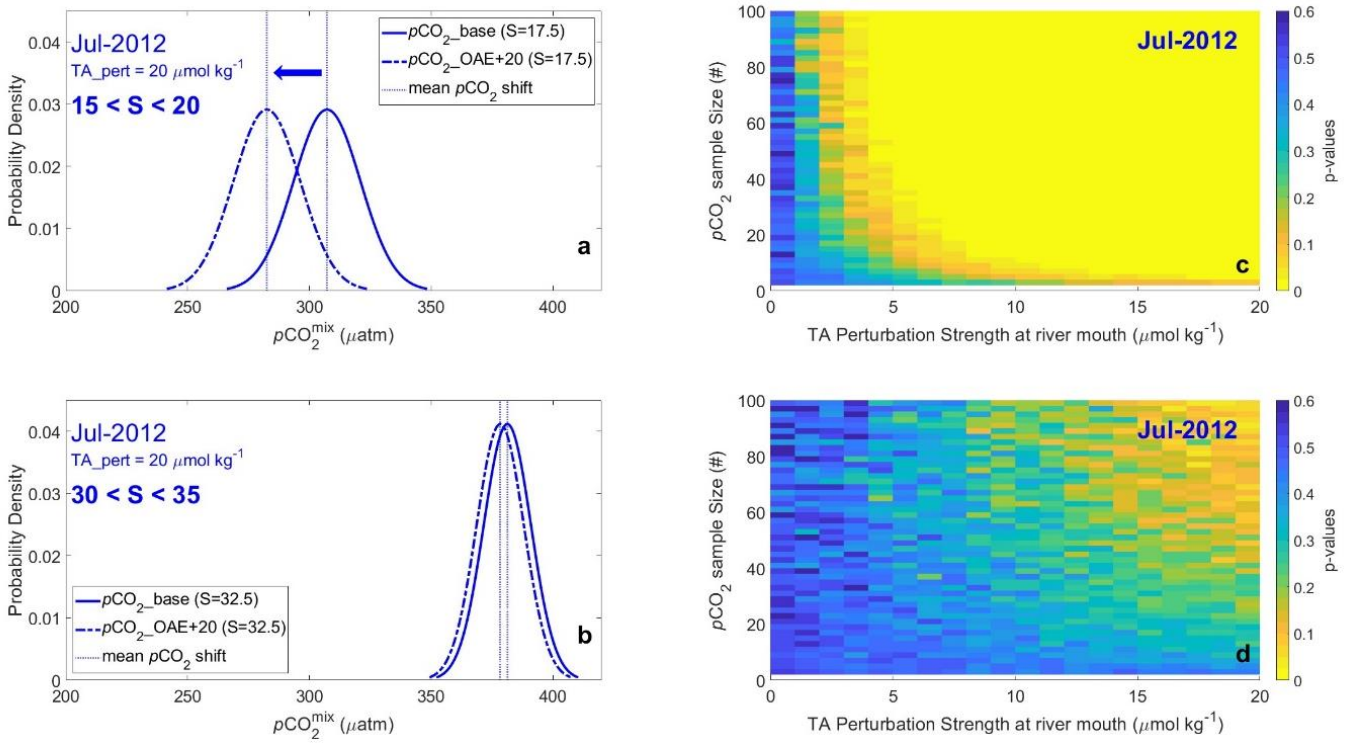

Figure S8. Detectability of OAE-induced pCO_2 variation at different salinity ranges of the plume water. (**a**). The theoretical shift of plume pCO_2 (μatm) distributions at 15 < SSS < 20, as a result of a TA perturbation of 20 μmol kg^{-1} at the river mouth. Black lines indicate the baseline pCO_2 calculated from the river and ocean carbonate endmembers at SSS = 17.5 (following the mixing curve shown in Figure S3b). The standard deviation of the baseline pCO_2 distribution is calculated from the root-mean-square error of pCO_2 residual values for 15 < SSS < 20, described in Figure S7. The mean of the pCO_2 in the perturbation scenarios (dash-dot lines) are calculated from perturbed TA and DIC values that follow the dash-dot line in Figure S3b. (**a**). Similar to (a) but for the salinity range of 30 < SSS < 35. (**c**)(**d**). The p-value plots from t-tests simulated between baseline and perturbed pCO_2 in the plume, induced by TA perturbation scenarios at various sample sizes and perturbation strengths for 15 < SSS < 20 and 30 < SSS < 35, respectively, in July 2012. Areas in yellow ($p < 0.1$) indicate conditions where an analyst would conclude that the TA perturbation was detected through pCO_2 relative to its baseline condition with 90% certainty.

Reference in Supplemental Materials

Mu, L., Gomes, H. do R., Burns, S. M., Goes, J. I., Coles, V. J., Rezende, C. E., Thompson, F. L., Moura, R. L., Page, B., and Yager, P. L.: Temporal Variability of Air-Sea CO2 flux in the Western Tropical North Atlantic Influenced by the Amazon River Plume, Global Biogeochem. Cy., 35, e2020GB006798, https://doi.org/10.1029/2020GB006798, 2021.

Mu, L., Richey, J. E., Ward, N. D., Krusche, A. V., Montebelo, A, Rezende, C. E., Medeiros, P. M., Page, B. P., and Yager, P. L.: Carbonate and nutrient contributions from the Amazon River to the western tropical North Atlantic Ocean, Global Biogeochem. Cy., in revision, 2023.

Ward, N. D., Krusche, A. V., Sawakuchi, H. O., Brito, D. C., Cunha, A. C., Moura, J. M. S., da Silva, R., Yager, P. L., Keil, R. G., and Richey, J. E.: The compositional evolution of dissolved and particulate organic matter along the lower Amazon River—Óbidos to the ocean, Mar. Chem., 177, 244–256, https://doi.org/10.1016/j.marchem.2015.06.013, 2015.